

The simulation of switching in polycrystalline ferroelectric ceramics

Stephen C. Hwang

Materials Department, University of California, Santa Barbara, California 93106-5050

John E. Huber

Cambridge University Engineering Department, Trumpington Street, Cambridge CB2 1PZ, United Kingdom

Robert M. McMeeking^{a)}

Materials Department, University of California, Santa Barbara, California 93106-5050

Norman A. Fleck

Cambridge University Engineering Department, Trumpington Street, Cambridge CB2 1PZ, United Kingdom

(Received 21 April 1997; accepted for publication 29 April 1998)

A polarization switching model for polycrystalline ferroelectric ceramics has been developed. It is assumed that a single ferroelectric crystallite in a ceramic, which is subjected to an electric field and/or a stress, undergoes a complete polarization change and a corresponding strain change if the resulting reduction in potential energy exceeds a critical value per unit volume of switching material. The crystallite's switch causes a change in the interaction of its field and stress with the surrounding crystallites, which is modeled by the Eshelby inclusion method to provide a mean field estimate of the effect. Thus the model accounts for the effects of the mean electric and stress fields arising from the constraints presented by surrounding crystallites as well as the externally applied mechanical and electrical loads. The switching response of the ceramic polycrystal is obtained by averaging over the behavior of a large number of randomly oriented crystallites. The model, along with the linear dielectric, elastic, and piezoelectric behavior of the material, is implemented in a computer simulation. A fit to experimental electric displacement versus electric field, strain versus electric field, and strain versus stress curves of a ceramic lead lanthanum zirconate titanate PLZT at room temperature is used to obtain material parameters. The model then successfully predicts the electric displacement and strain hysteresis loops for the PLZT under varying electric fields with a constant applied stress. © 1998 American Institute of Physics. [S0021-8979(98)06015-0]

I. INTRODUCTION

Switching is the source of the butterfly shaped strain versus electric field curves and the corresponding electric displacement versus electric field hysteresis loops for ferroelectric ceramics.¹ Such hysteresis loops for an 8/65/35 lead lanthanum zirconate titanate (PLZT) polycrystalline ceramic at room temperature are shown in Figs. 1 and 2. Given that switching is the only source of nonlinear strain and electric displacement response for a polycrystalline ferroelectric ceramic, it should be possible to model experimentally obtained hysteresis loops by a combination of a switching criterion for individual crystallites and the linear response of the polycrystal.²⁻⁴ Such a model would be useful for predicting the nonlinear response of the material under multiaxial states of mechanical and electrical loading and for guiding the development of phenomenological constitutive laws by augmenting the limited data from experiments.^{1-3,5-9} An additional motivation is to explore how well a mean field theory, with the in-built assumption that crystallites are always completely polarized in their current orientation or in their new orientation after transformation, simulates the observed behavior during switching of a polycrystalline ferroelectric ceramic.

An attempt to develop such a model is presented in this article. It is assumed that each crystallite in the ceramic is tetragonal with six possible orientations for polarization.¹ (It should be noted, however, that other crystallographies such as rhombohedral could be implemented easily in the model.) The net polarization and strain of the polycrystal is the volume average over all crystallites of the local values. The energy barrier to 90° switching for an individual crystallite is taken to be much less than the barrier to 180° switching. A switch is then assumed to take place in an individual crystallite when the magnitude of the reduction in potential energy of the system due to the switch equals the size of the energy barrier to the switch. Thus this version of the model neglects thermal activation and the associated rate effects and is for cases where the external fields are varied very slowly compared to the relaxation rates for domain wall processes. However, we assume that switching in crystallites is opposed by finite energy barriers capable of being easily overcome by applied fields.

From ample experimental evidence,^{1,5,10-12} we conclude that switching occurs by domain wall motion. However, as noted above, we explore a model in which complete switching takes place in a crystallite when it meets the critical condition for repolarization. We do not follow the domain wall as it traverses the crystallite but only compare the beginning and end points of the process of complete switching

^{a)} Author to whom correspondence should be addressed.

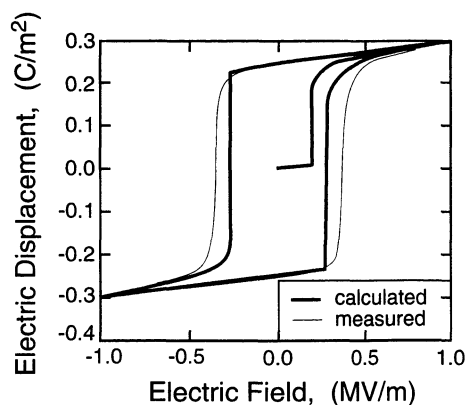


FIG. 1. Simulated and measured 8/65/35 PLZT electric displacement vs electric field hysteresis loops with no applied stress.

of the crystallite. Thus, the domain wall is considered to move very quickly through the crystallite. This seems reasonable given the high mobility of domain walls^{1,5,10,11} and the fact that the applied loads are considered to vary slowly. The assumption of complete switching for a crystallite requires us to use the criterion discussed above that the energy change upon transformation equals a critical value. Other criteria such as the meeting of a critical electric field in the crystallite are unsuitable. They lead to the immediate reversal of many switches due to the large depolarization fields (electrical and mechanical) generated in the crystallites after the initial transformation. Our experience with the model has shown us that only if the total energy reduction of the system is equal to a critical value will all the switches be stable and not immediately reverse themselves. Thus our criterion for switching seems to be the only suitable one given that a crystallite is assumed to switch itself entirely upon transformation.

The calculation of the reduction of the potential energy due to a switch is carried out by modeling the crystallite as a spherical inclusion in an infinite homogeneous matrix representing the polycrystalline ceramic. Such mean field theories have been widely used to model mechanical behavior at the macroscopic level,¹³⁻¹⁸ including the plasticity of polycrystals. Recently, Arlt¹⁹ has used a mean field theory as the

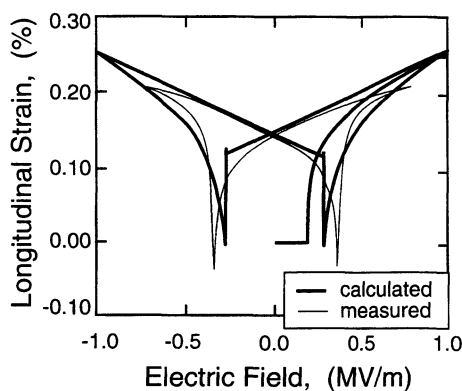


FIG. 2. Simulated and measured 8/65/35 PLZT longitudinal strain vs electric field butterfly loops with no applied stress.

basis of a model for the switching of ferroelectric ceramic polycrystals, but using only dielectric polarization and electrostatics without any mechanical features in the theory. In contrast, we wish to account for the effects of polarization strain in addition to the electrical effects and to develop a model for polycrystalline ferroelectric switching analogous to those already in place for polycrystalline plasticity.^{13-15,18} In our case, the inclusion is assumed to be a single crystallite switching all at once when the transformation takes place, as noted above. One contribution to the reduction in potential energy of the system upon switching is due to the interaction of the switch with the applied fields. A second contribution is the change in stored energy of matrix constraint due to the complete reorientation of the electrical and mechanical polarization of the inclusion. The constraint of the matrix on the inclusion is computed as if it were enforced invariantly by the linear properties of the material, but with piezoelectricity omitted. However, material property values for the matrix are chosen for the energy change calculation which reduce the effect of the constraint compared to that which would be enforced by the measured linear dielectric permittivity and elastic modulus of the ceramic polycrystal. This softness of the matrix yields a better fit with experimental measurements of hysteresis and butterfly loops, but can also be rationalized as a consequence of the on-going switching of the matrix material. Such an approach is a well established procedure in the modeling of plasticity in polycrystals, where the full elastic constraint used in the method of Kroener-Budiansky-Wu^{13,14} is well known to be too stiff when inelastic straining is widespread throughout the crystallites.^{15,18} The softness may also be due to the presence of pores, cracks, electrodes, and free surfaces near the domains which initiate switching in a heterogeneous material.

It is well known that the vast majority of crystallites in a ferroelectric polycrystal in the initial state after cooling down through the Curie temperature become stabilized due to the screening of polarization charges by free charge carriers and because of domain, twinning, and strain coordination with neighbors.¹ The mean effect of the stabilization is not zero and cannot be attributed to random spatial fluctuation of electric and mechanical fields. The effects of this stabilization contribute to the energy increase during the switching process and may be roughly described by the introduction of an additional energy barrier hindering it. The magnitude of the energy barrier to switching used in our model is an adjustable parameter and is assumed to take into account this stabilization feature.

In fitting our model to the data, we have found it necessary to weight the potential energy change due to the transformation strain more heavily than the potential energy change due to the electrical polarization. This makes switching driven by applied stress easier to achieve and the fit to the data is then better. It is possible that this step is made necessary by the approximations introduced when the interactions among simultaneously and progressively switching crystallites are represented by a mean field theory having a fixed level of isotropic constraint on crystallites which completely transform during repolarization. In conjunction with this, the omission of piezoelectricity in the constraint calcu-

lation may have contributed to the requirement for weighting one of the terms over the other. In light of these points, the resulting weighting of the contribution of the transformation strain to the potential energy change by 140% is significant but not excessive. In any case, the numerical results and the degree of empirical adjustment which has been introduced into the model are indicators of the relative validity and success of this particular method of simulating polycrystalline ferroelectric switching.

The simulations are carried out with a large number of crystallites having initially random tetragonality. The starting point for the polycrystal is therefore one of zero average polarization and this state is chosen as the datum for electric displacement and strain. The applied electrical and stress fields are then gradually increased and later reversed. The behavior is followed incrementally by permitting in each step the switching of the crystallites most favored in the sense of the driving force exceeding the barrier. The load is kept constant until all the energetically favorable crystallites switch. However, only a very small number are allowed to transform initially in each update. The step sizes are therefore chosen to be small and the number of increments in a simulation is large. The macroscopic polarization and strain are computed by simple number averaging over all crystallites which are assumed to have equal volume. This average includes the linearly produced contributions (i.e., dielectricity, elasticity, and piezoelectricity) as well as the nonlinear amounts caused by switching.

The parameters of the model are chosen from empirical constants or by fitting the results of the model to the experiment. Predictions of behavior not used to obtain the fit are then made and the result is fairly successful. A PLZT 8/65/35, which is mostly rhombohedral, has been used in this exercise despite the simulation being carried out with the assumption that the material is tetragonal. Because of the large number of crystallites used in the calculations, the model is still physically justifiable for this case, with the 90° tetragonal switches providing a reasonable representation of the ~70° and ~110° switches in the rhombohedral phase.

II. PROBLEM DESCRIPTION

The ceramic volume V is considered to be composed of a large number of equiaxed crystallites of initially random tetragonal orientation. The crystallites are bonded together perfectly at their boundaries with no extrinsic charge present anywhere within the ceramic. The exact problem, therefore, has an electric displacement \mathbf{D} satisfying in V

$$\partial D_i / \partial x_i = 0 \quad (1)$$

along with the continuity condition

$$n_i [D_i] = 0 \quad (2)$$

across the crystallite boundaries where \mathbf{x} is position, \mathbf{n} is the outward unit normal to the boundary, and the symbol $[]$ denotes a jump in the quantity contained within it. All components of vectors and tensors are referred to a common fixed Cartesian coordinate system. Mechanical equilibrium requires that in V

$$\partial \sigma_{ij} / \partial x_i = 0, \quad (3)$$

and

$$n_i [|\sigma_{ij}|] = 0 \quad (4)$$

across crystallite boundaries, where $\boldsymbol{\sigma}$ is the mechanical stress.

Each crystallite obeys a constitutive law for the electric displacement given by

$$D_i = \epsilon_{ij} E_j + d_{ikt} \sigma_{kl} + P_i^r, \quad (5)$$

where $\boldsymbol{\epsilon}$ is the tensor of dielectric permittivities, \mathbf{d} is the tensor of piezoelectric coefficients and \mathbf{P}^r is the spontaneous polarization of the crystallite with magnitude P_0 . The electric field vector, \mathbf{E} is given by

$$E_i = -\partial \Phi / \partial x_i, \quad (6)$$

where Φ is the potential. The c axis of the tetragonal unit cell is parallel to \mathbf{P}^r . The strain, e_{ij} , in a crystallite is defined in terms of the displacement, \mathbf{u} , in the usual manner

$$e_{ij} = (\partial u_i / \partial x_j + \partial u_j / \partial x_i) / 2 \quad (7)$$

and satisfies the constitutive law

$$e_{ij} = d_{kij} E_k + s_{ijlm} \sigma_{lm} + e_{ij}^r, \quad (8)$$

where \mathbf{s} is the tensor of elastic compliances and \mathbf{e}^r is the spontaneous strain of the tetragonal unit cell measured from a cubic datum. Thus, \mathbf{e}^r has principal values

$$e_{\text{III}} = \frac{c - a_0}{a_0} \quad (9)$$

and

$$e_{\text{I}} = e_{\text{II}} = \frac{a - a_0}{a_0}, \quad (10)$$

where a and c are the lattice parameters of the tetragonal unit cell and a_0 is the lattice parameter of the cubic unit cell above the Curie temperature. Later, however, we will assume that $e_{\text{I}} = e_{\text{II}} = -e_{\text{III}}/2$ with $e_{\text{III}} = e_0$ so that the tetragonal unit cell has the same volume as the cubic cell. The principal directions of the spontaneous strain are the c axis (e_{III}) and the directions orthogonal to the c axis.

The dielectric permittivity, piezoelectric coefficient, and elasticity tensors in general are anisotropic with the polar axis determining the symmetries. The exact macroscopic properties of the ceramic are weighted or unweighted averages of the crystallite properties with the governing equations (1)–(4) taken into account. Standard methods are available to obtain approximate values for the macroscopic linear properties.^{16,17} However, linear properties are not the focus of this article. Instead the nonlinear behavior is of interest. Therefore, the problem is simplified by assuming $\boldsymbol{\epsilon}$ and \mathbf{s} to be isotropic and the same for every crystallite given by

$$\epsilon_{ij} = \epsilon \delta_{ij}, \quad (11)$$

where ϵ is the dielectric permittivity and

$$s_{ijkl} = \frac{1 + \nu}{Y} \delta_{ik} \delta_{jl} - \frac{\nu}{Y} \delta_{ij} \delta_{kl}, \quad (12)$$

where ν is Poisson's ratio and Y is Young's modulus. The calculation of the macroscopic linear properties for dielectric permittivity and elasticity is then simplified since they will also be equal to (11) and (12), respectively. With these assumptions, the dielectric permittivity and the elasticity of the polycrystalline ceramic will be isotropic even when it has a net polarization. The impact of this approximation in the modeling of uniaxial behavior will be diminished by choosing ϵ , ν , and Y to match the experimental data measured from uniaxial poling and stressing experiments on the polycrystalline ceramic.

The piezoelectric coefficient tensor for each crystallite, when referred to the coordinate system in which the positive x_3 axis is parallel to the positive polarization direction, has the positive valued component d_{333} . The other components of \mathbf{d} which are nonzero are assumed to be

$$d_{311} = d_{322} = -\frac{1}{2}d_{333}. \tag{13}$$

This is a somewhat simplified model for the piezoelectricity of a single crystallite. However, the neglected terms will contribute less significantly to the macroscopic average piezoelectric behavior of the transversely isotropic polycrystal, so their omission can be justified.

In the model, the nonlinear properties of the polycrystalline ceramic are determined by imposing a potential on the boundary of the ceramic which is consistent with a uniform electric field and tractions which are in equilibrium with a uniform stress. The resulting fields must then satisfy Eqs. (1)–(8) as well as the boundary conditions. The macroscopic remanent polarization is the volume average of the spontaneous polarization of the crystallites and the macroscopic remanent strain is the volume average of the spontaneous strain of each crystallite. Initially, the spontaneous polarizations are random so the macroscopic remanent polarization is zero as is the macroscopic remanent strain. As the electric field or the stress or both are increased, switching takes place and therefore, on average, the remanent polarization and the remanent strain can become nonzero.

A crystallite is assumed to switch when the reduction of potential energy of the system due to that switch is equal to a critical value, which can be considered to be equal to the energy barrier which must be overcome to achieve the switch. The potential energy of the system is^{20,21}

$$U = \int_V \frac{1}{2} [\sigma_{ij}(e_{ij} - e_{ij}^r) + E_i(D_i - P_i^r)] dV - \int_S T_i u_i dS - \int_S \Phi q dS, \tag{14}$$

where S is the exterior surface of V , \mathbf{T} is the mechanical traction on S , and q is the extrinsic charge surface density present on S . The form of (14) recognizes that the tractions \mathbf{T} and the potential Φ are specified everywhere on S . It has also been assumed that the electrostatic energy in regions external to V can be neglected. This can be justified usually for ferroelectrics because the dielectric permittivity is high compared to that of air. As a result, the electric displacement exterior to a ferroelectric is often very small compared to that within. In such a situation, the boundary condition on S is

$$q = -n_i D_i, \tag{15}$$

where \mathbf{n} is the exterior normal to S and \mathbf{D} is the electric displacement in V at the surface S . This condition arises because \mathbf{D} is neglected outside V and so $n_i[D_i] = -\hat{n}_i D_i$. However, this boundary condition must be used with care because it is invalid when there is significant electrostatic coupling through the external surface with another element or when there is self-coupling as through re-entrant corners, notches, or cracks.²²

We assume that one crystallite switches at a time so that a change in the potential energy can be ascribed to the repolarization of an individual crystallite with the traction and potential on S held fixed. The change ΔU occurs because \mathbf{P}^r in the switching crystallite will be reoriented and possibly so will \mathbf{e}^r . The requirement that Eqs. (1)–(8) must still be satisfied after the switch will lead to changes in all the terms in U except \mathbf{T} and Φ on S which are fixed. The criterion for the switch is therefore

$$-\Delta U = V_c \Delta \Psi_c, \tag{16}$$

where V_c is the volume of the switching crystallite and $\Delta \Psi_c$ is the energy barrier against the switch per unit volume. In this work, we assume that the energy barrier to a 90° switch $\Delta \Psi_c^{90}$ is different from the barrier to a 180° switch $\Delta \Psi_c^{180}$.

III. INCLUSION MODEL

To estimate the change of potential energy for a switch, we approximate the problem stated above as a spherical inclusion which is switching embedded in a nontransforming homogeneous matrix with a fixed remanent polarization \mathbf{P}^{rm} and strain \mathbf{e}^{rm} . The inclusion undergoes a change in spontaneous polarization $\Delta \mathbf{P}^r$ and strain $\Delta \mathbf{e}^r$ while the applied stress $\boldsymbol{\sigma}^A$ and electric field \mathbf{E}^A are held fixed at infinity. This problem is related to that for an elastic inclusion solved by Eshelby^{21,23} and our treatment will take advantage of his insights. There is equivalence also with the problem of a cavity in a dielectric medium.²⁰

The piezoelectric inclusion has been the subject of several treatments.^{24–27} The results are quite complicated and are not readily used for repetitive computation of the potential energy of several thousand inclusions. When the problem is approximated as a piezoelectric inclusion in an isotropic matrix, the results are more tractable but still complicated.²⁸ The simplest version of the problem which retains the physical features in a reasonable fashion is one in which the piezoelectric terms are neglected completely. In this treatment, the potential energy due to the inclusion is that of an isotropic elastic inclusion with a transformation strain in a homogeneous isotropic elastic matrix with a different residual strain plus the energy of an isotropic electrostatic inclusion with a spontaneous polarization in an isotropic matrix with a remanent polarization different from the spontaneous polarization of the inclusion. Following Eshelby^{21,23} and Deeg,²⁴ McMeeking and Hwang²⁸ have shown this to be

$$U = U_0 + U_I, \tag{17}$$

where U_0 is U from Eq. (14) evaluated with \mathbf{e}^r and \mathbf{P}^r uniform everywhere in V and

$$\begin{aligned}
U_I = V_I & \left[-\sigma_{ij}^A (e_{ij}^{ri} - e_{ij}^{rm}) - E_i^A (P_i^{ri} - P_i^{rm}) \right. \\
& + \frac{(7-5\nu)Y}{30(1-\nu^2)} (e_{ij}^{ri} - e_{ij}^{rm})(e_{ij}^{ri} - e_{ij}^{rm}) \\
& \left. + \frac{1}{6\epsilon} (P_i^{ri} - P_i^{rm})(P_i^{ri} - P_i^{rm}) \right], \quad (18)
\end{aligned}$$

where V_I is the volume of the spherical inclusion. Here, U_0 is the potential energy of the solid when the inclusion has a spontaneous polarization and strain equal to the remanent polarization and strain of the matrix. The contribution U_I arises from the differences between the spontaneous polarization and strain in the inclusion and the remanent polarization and strain in the matrix. The first two terms on the right hand side of Eq. (18) are the interaction of the transformation strain, $\mathbf{e}^{ri} - \mathbf{e}^{rm}$ with the applied stress and the transformation polarization $\mathbf{P}^{ri} - \mathbf{P}^{rm}$ with the applied field. The third term is the elastic energy due to the transformation strain in an isotropic elastic body without any applied load, as given by Eshelby.^{21,23} The fourth term is the electrostatic energy due to the transformation polarization in an isotropic dielectric free of field at infinity and can be deduced from the solution for a spherical cavity in an isotropic dielectric.²⁰ Therefore, Eq. (18) accounts for the misfit of inclusion strain and polarization but does not account for the difference in electromechanical properties (i.e., modulus, permittivity, and piezoelectricity) between the inclusion and matrix. A fuller although incomplete account of the additional terms is given by McMeeking and Hwang.²⁸

When the inclusion switches, U_0 is unaltered but U_I changes to $U_I + \Delta U$. The change occurs because the inclusion spontaneous polarization becomes a new value, $\mathbf{P}^{ri} + \Delta \mathbf{P}^{ri}$. At the same time, the inclusion spontaneous strain changes to $\mathbf{e}^{ri} + \Delta \mathbf{e}^{ri}$, with the increment $\Delta \mathbf{e}^{ri}$ zero if a 180° switch is involved. Consequently,

$$\begin{aligned}
\Delta U = V_I & \left[-\sigma_{ij}^A \Delta e_{ij}^{ri} - E_i^A \Delta P_i^{ri} \right. \\
& + \frac{(7-5\nu)Y}{15(1-\nu^2)} \left(e_{ij}^{ri} - e_{ij}^{rm} + \frac{1}{2} \Delta e_{ij}^{ri} \right) \Delta e_{ij}^{ri} \\
& \left. + \frac{1}{3\epsilon} \left(P_i^{ri} - P_i^{rm} + \frac{1}{2} \Delta P_i^{ri} \right) \Delta P_i^{ri} \right], \quad (19)
\end{aligned}$$

Consider the case of 90° switching and let $P_1^{ri} = P_0$, whereas $P_2^{ri} = P_3^{ri} = 0$ (i.e., the inclusion polarization is initially aligned with the positive x_1 direction). Let the inclusion polarization switch to the positive x_3 direction so that $\Delta P_1^{ri} = -P_0$, $\Delta P_3^{ri} = P_0$, and $\Delta P_2^{ri} = 0$. As a consequence

$$(P_i^{ri} + \frac{1}{2} \Delta P_i^{ri}) \Delta P_i^{ri} = 0. \quad (20)$$

For the same switch, assume initially that $e_{11}^{ri} = e_0$ and $e_{22}^{ri} = e_{33}^{ri} = -\frac{1}{2}e_0$ with other terms in $e_{ij}^{ri} = 0$. Therefore, $\Delta e_{11}^{ri} = -\frac{3}{2}e_0$ and $\Delta e_{33}^{ri} = \frac{3}{2}e_0$ with $\Delta e_{ij}^{ri} = 0$, otherwise. It follows that

$$(e_{ij}^{ri} + \frac{1}{2} \Delta e_{ij}^{ri}) \Delta e_{ij}^{ri} = 0. \quad (21)$$

Although illustrated for a particular case, Eqs. (20) and (21) are in fact general. Therefore, the potential energy change due to a 90° switch of the inclusion is

$$\begin{aligned}
\Delta U = -V_I & \left[\left(\sigma_{ij}^A + \frac{(7-5\nu)Y e_{ij}^{rm}}{15(1-\nu^2)} \right) \Delta e_{ij}^{ri} \right. \\
& \left. + \left(E_i^A + \frac{1}{3\epsilon} P_i^{rm} \right) \Delta P_i^{ri} \right]. \quad (22)
\end{aligned}$$

When a 180° switch takes place, $\Delta \mathbf{P}^{ri} = -2\mathbf{P}^{ri}$ and $\Delta \mathbf{e}^{ri}$ is zero; ΔU is again given by Eq. (22).

IV. NUMERICAL SIMULATION

The model for ferroelectric behavior is implemented in a numerical simulation with several thousand crystallites. A random number generator is used to create the principal axes of the initial tetragonal unit cell of each crystallite with a spontaneous strain e_0 in the c axis direction and $-e_0/2$ in the other two principal directions. A spontaneous polarization of magnitude P_0 is assigned randomly to one of the two directions parallel to the c axis of the unit cell. The components of the spontaneous polarization and strain of each crystallite are calculated in a fixed Cartesian coordinate system common to the aggregate of crystallites. These components will be referred to throughout the discussion below. With \mathbf{m} being a unit vector in the polarization direction of the crystallite, the components of the remanent polarization for that crystallite are given by

$$P_i^r = P_0 m_i \quad (23)$$

and the remanent strain is

$$e_{ij}^r = \frac{1}{2} e_0 (3 m_i m_j - \delta_{ij}). \quad (24)$$

The macroscopic polarization of the aggregate is computed as the volume average of the polarization in the crystallites. Since each crystallite is assumed to have the same volume V_I , the volume average can be computed as a simple arithmetic average of the polarization vector components over all crystallites. Similarly, the macroscopic strain of the aggregate is the volume average of the crystallite strains, deduced by a simple arithmetic average over all crystallites. Thus, the initial remanent polarization and strain of the aggregate is zero, or nearly zero because of the finite number of crystallites involved in the random simulation. Similarly, the linear contributions to the electric displacement D_i and strain e_{ij} are zero initially because the applied field and stress are zero initially.

The applied field, or the stress, or both (referred to jointly as the load) are gradually introduced. After a small increment of load is applied, each crystallite is checked to see if it has met the switching criterion. The expression for ΔU given by Eq. (22) is substituted into the switching criterion [Eq. (16)] and is modified to the form

$$\alpha \left(\sigma_{ij}^A + \frac{2}{5} \bar{Y} e_{ij}^{rm} \right) \Delta e_{ij}^{ri} + \left(E_i^A + \frac{1}{3\epsilon} P_i^{rm} \right) \Delta P_i^{ri} \geq 2 \bar{E}_0 P_0 \quad (25)$$

Here, the energy $\Delta \Psi_c$ is rewritten as $2 \bar{E}_0 P_0$, where \bar{E}_0 is an effective coercive field magnitude. The value of \bar{E}_0 is chosen

to provide a best fit of the simulation results to experimental data. (Note: \bar{E}_0^{90} for a 90° switch is different from \bar{E}_0^{180} for a 180° switch.) α is a weighting parameter differentiating the mechanical and the electrical driven switching. A value of α greater than unity is chosen in order to encourage stress induced switching. This requirement has been observed previously by Hwang *et al.*³ The term \bar{Y} is an effective modulus which will be also chosen to provide a best fit of the numerical simulation to experimental data for hysteresis loops as discussed below. Poisson's ratio is approximated as 1/2 in Eq. (22), giving rise to the numerical factor of 2/5 in Eq. (25). Similarly, $\bar{\epsilon}$ is an effective dielectric permittivity chosen to provide the best fit to experimental hysteresis data. The unbarred terms Y and ϵ are reserved for the linear elastic modulus and linear dielectric permittivity of crystallites. The values of \bar{Y} and $\bar{\epsilon}$ used in the switching criterion are permitted to differ from Y and ϵ . The latter quantities are chosen to agree with measured values of the linear elastic modulus and linear dielectric permittivity of poled polycrystalline ferroelectric ceramics.

Care must be exerted in implementing the criterion expressed in Eq. (25), due to the possibility of nonunique switching. For each crystallite the tetragonal symmetry dictates five possible switches. For a given load increment, the switch which is taken to occur is that associated with the greatest value of the left hand side of Eq. (25).

After all possible switches have been identified and made, the macroscopic remanent polarization and strain for the aggregate of crystallites is recomputed by averaging over the crystallites. These values are also assigned as new values of the matrix remanent polarization and strain (i.e., \mathbf{P}^m and \mathbf{e}^m) for use in subsequent calculations with Eq. (25) [Note: on the first step, Eq. (25) is used with $\mathbf{P}^m = \mathbf{e}^m = 0$]. With \mathbf{P}^m and \mathbf{e}^m updated, further switching is allowed to occur without increase of the load. This process is repeated until no more crystallites will switch. The load is then incremented and Eq. (25) used to select further switches. The increments of load are chosen so that only a few crystallites switch at any given stage. However, many crystallites can follow the few crystallites already switched at the same load. This is the same autocatalytic effect observed in the experiments. Once a few crystallites trigger switching, then other crystallites follow suit. Thus, many crystallites can switch at the same load.

At each stage, the linear contribution to the electric displacement and the strain is computed from the linear terms in Eqs. (5) and (8), with Eqs. (11) and (12) used for the elastic modulus and dielectric permittivity tensor and the remanent quantities given by Eqs. (23) and (24). With the piezoelectric coefficient tensor having the form of (13), it can be stated as

$$d_{ijk} = \frac{1}{2} d_{33} m_i (3m_j m_k - \delta_{jk}), \quad (26)$$

where d_{33} is the axial piezoelectric coefficient for the crystallite.¹ The applied electric field \mathbf{E}^A is used for \mathbf{E} in Eqs. (5) and (8) and the applied stress $\boldsymbol{\sigma}^A$ is used for $\boldsymbol{\sigma}$. The macroscopic electric displacement for the aggregate of crystallites is then computed by averaging the electric displacement over all crystallites and the macroscopic strain for the aggregate is obtained by averaging the crystallite strains. The

assumed homogeneity of linear properties over all crystallites obviates the need to use local crystallite values for $\boldsymbol{\sigma}$ and \mathbf{E} in Eqs. (5) and (8).

V. RESULTS

The simulation is fitted to experimental data for polycrystalline 8/65/35 PLZT with 5 μm grain size. Hysteresis loops were obtained for a 10 mm cube of the material driven by loads cycled in triangle shaped waves at 0.02 Hz. The experiments and results were described in a previous paper by Hwang *et al.*³

It is found that a best fit can be obtained with $\bar{E}_0^{90} = 0.13$ MV/m, $\bar{E}_0^{180} = 1.0$ MV/m (\bar{E}_0^{180} can be any large value discouraging any 180° switch) $\bar{\epsilon} = 0.80$ $\mu\text{F}/\text{m}$, $\bar{Y} = 7.5$ GPa, and $\alpha = 1.4$. These values differ substantially from the nominal magnitudes of coercive field, dielectric permittivity, and Young's modulus for PLZT. This discrepancy will be discussed later. With the given values for these constants, a simulation with 5000 crystallites gives reproducible results. For example, the initial remanent polarization of the aggregate is typically less than 0.1% of the saturated remanent polarization of the polycrystal; also, the numerical results for a simulation for a given random set of 5000 crystallites are within 5% of the values for other simulations based on a different random set of 5000. These characteristics are improved if a larger number of crystallites is used, but 5000 is considered to be an effective number in the compromise between reproducibility and computer effort.

Other values used for parameters are $P_0 = 0.30$ C/m², $e_0 = 0.0028$, $\epsilon = 0.05625$ $\mu\text{F}/\text{m}$, $Y = 34$ GPa, and $d_{33} = 2.376 \times 10^{-9}$ m/V. The last two values have been chosen to provide good agreement of the model in the linear response regime with the overall shape of the hysteresis loops.

A. Electric displacement versus electric field at zero stress

Figure 1 shows the electric displacement versus electric field hysteresis loops with experiments represented by the thin line and calculations by the bold line. The simulation shows very good agreement with the experiments, confirming the effectiveness of the choice of fitting parameters. At a higher magnitude of the electric field, the simulated curves do not match the measured ones well. This feature arises because of a nonlinear response of the ferroelectric in the experiments. We believe that this is due to a diminution of the dielectric permittivity as the field magnitude increases. In other words, it appears that the "linear" dielectric response saturates at a high field in the experiments. This effect is not included in the simulations.

A characteristic of the measured curves which is not captured well in the simulations is the gradual change of the remanent polarization at the beginning of and during switching. The simulations give a much more abrupt transition from saturation of the remanent polarization to switching and a steeper slope during switching. Improvements in this aspect of the simulation cannot be made without compromising other aspects of the agreement between the simulated curves and the measured ones.

It should be noted that the experimental loops shown in Fig. 1 and in all other figures are the repeatable curves obtained after several transient cycles of load. The experiment and the simulation both start at zero electric field and zero electric displacement. For the first few cycles, the loops have different shapes. Eventually the hysteresis curves settle down to those displayed in the figures. The initial transient loops have been omitted in all figures except the simulated ones in Figs. 1 and 2. Initially, switching commences at ~ 0.2 MV/m. However, once the ceramic is poled, switching occurs consistently at ~ 0.3 MV/m due to the influence of matrix constraints. In all plots, the data used as the starting point of the simulation are zero electric field, zero electric displacement, zero strain, and zero mechanical stress.

B. Strain versus electric field at zero stress

The fitting of the strain-electric field butterfly loop of the simulations to the experiments is the most critical aspect of selecting the three constants \bar{E}_0^{90} , \bar{Y} , and $\bar{\epsilon}$ in the model. The result is shown in Fig. 2. This behavior occurs simultaneously with that depicted in Fig. 1. In obtaining the best fit, it was important to ensure that the simulation reproduced the long narrow tails of the butterfly loop associated with switching as well as the remanent strain at zero electric field. The tails are the result of consecutive 90° switchings for given crystallites. The first switch contributes to a reduction in the axial strain. Such switches occur first so that the axial strain for the aggregate goes to zero as shown in simulations and even becomes negative as in experiments (recall that the datum for strain is the original shape of the unpoled polycrystalline aggregate). The second 90° switches then start to occur as the electric field is changed further and the axial strain recovers to the levels present in the fully poled material.

In a previous effort to simulate ferroelectric behavior,³ the long tails on the butterfly loops could not be reproduced and there was considerable positive remanent strain in the aggregate even when the polarization had disappeared. This feature in the previous simulation was due to the fact that 180° switching was preferred numerically even though 90° switching was permitted. The difference in the previous simulation was the low barrier to 180° switching and the omission of the constraint terms in Eq. (25) (i.e., \bar{Y} was set to zero and $\bar{\epsilon}$ to ∞) so that only the work done by the applied load (σ^A and E^A) was considered to contribute to the reduction of potential energy of the system upon transformation of a crystallite. When the barrier to 180° switching is raised and the process occurs by 90° switches alone, the shape of the tails of the butterfly loops is improved. However, the effect of matrix constraint is needed also to produce realistic loops. After a first 90° switch, many crystallites are locked into their new states by matrix constraint and are unable to undergo a second 90° switch until the applied load is changed. The second 90° switch does not occur immediately because of the dielectric energy penalty when a crystallite polarization opposes the average polarization. Thus, an increase in field magnitude is required before the second 90° switch occurs in a crystallite. This illustrates the point that the constraint terms in Eq. (25) encourage crystallites to match

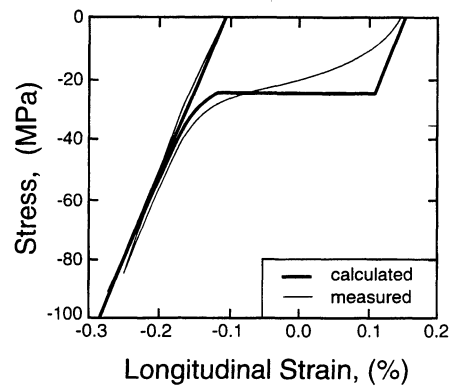


FIG. 3. Simulated and measured 8/65/35 PLZT stress vs strain curves for a poled ceramic with no applied electric field.

themselves as much as possible to the average behavior, introducing an autocatalytic feature to the behavior. Once one crystallite executes a 90° switch, other crystallites will be more susceptible to 90° switching and a coordinated process of transformation then ensues.

The favoring of 90° switching in the simulations presented in this article is due to mismatch constraint between a given crystallite and the matrix, with the matrix representing average aggregate behavior. However, we have also found in separate work²⁸ that the difference in linear piezoelectric properties between crystallite and matrix can cause a first 90° switch to occur more readily than a second, which then takes place only after the applied load is further increased. Therefore, even though the piezoelectric property mismatch energy²⁸ has been omitted from Eq. (25), the constraint terms in Eq. (25) can be viewed as substituting for this piezoelectric effect in the model as well as representing the mismatch of shape and remanent polarization between the crystallite and the matrix.

C. Stress versus strain at zero electric field

The experiment and simulation for this are carried out on a poled ceramic. A poled ceramic is one which has been taken through several cycles of high electric field reversal until a repetitive hysteresis behavior is achieved. That is, the procedure is followed which produces the repetitive loops shown in Figs. 1 and 2. The electric field is then removed, so that the polycrystalline ceramic has a net remanent polarization (approximately 0.24 C/m² in magnitude) and a net remanent strain (approximately 0.14%).

A compressive mechanical stress is then applied to the ceramic parallel to the polarization and later removed. The result is shown in Fig. 3. Although the simulation gives a poor reproduction of the details of the shape of the measured curve, the basic shape and magnitude of the simulated curve are satisfactory. This feature is significant, because in the previous effort³ to simulate these curves, the strength of the material during stress driven depolarization was greatly overestimated. The magnitude of \bar{E}_0^{90} seems to be largely responsible. The low value for \bar{E}_0^{90} , along with a stress driven term enhanced by α as used in the simulation depicted in Fig. 3, makes stress driven depolarization relatively easy to achieve,

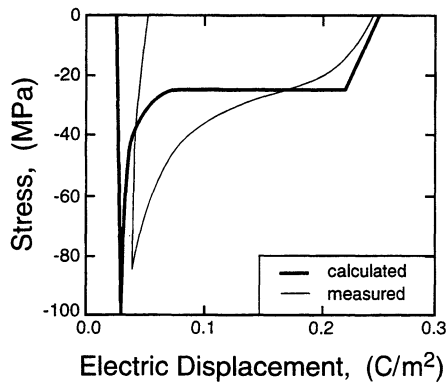


FIG. 4. Simulated and measured 8/65/35 PLZT stress vs electric displacement curves for a poled ceramic with no applied electric field.

without degrading the quality of the simulation of electric field driven polarization and repolarization. The prediction of remanent strain after removal of the stress is remarkably good.

The simulated stress–strain curve in Fig. 3 shows a more abrupt transition to depolarization than the measured curve which is quite gradual. This suggests that the effective initial resistance to stress driven depolarization is even lower than we infer from our simulation. Improvement of this error could not be achieved without degrading the agreement achieved for other experimental data.

D. Stress versus electric displacement at zero electric field

During the application of compressive mechanical stress to the poled ceramic, depolarization takes place. This leads to the curves shown in Fig. 4, which occur simultaneously with those shown in Fig. 3. It appears that the simulation captures the stress–depolarization effect better in terms of strain than in terms of electric displacement (i.e., compare Figs. 3 and 4).

VI. PREDICTIONS

The simulation results presented in the previous section are simply the consequence of the fitting procedure. The agreement between the simulations and experimental data is satisfying, but does not represent a prediction of additional behavior. Further simulations are carried out in this section to predict other experimental data. The ten empirical parameters (\bar{E}_0^{90} , \bar{E}_0^{180} , \bar{Y} , $\bar{\epsilon}$, α , e_0 , P_0 , Y , ϵ , and d_{33}) are kept at the same values as before to carry out these additional calculations.

The poled ceramic (i.e., one having the repetitive hysteresis loops shown in Figs. 1 and 2) is used as the initial state for further simulations. A compressive stress of a chosen magnitude is applied parallel to the polarization direction and held fixed. An electric field parallel to the applied stress is then introduced and cycled between positive and negative limits. The results are shown in Figs. 5(a), 5(b), 6(a) and 6(b). These are repeatable loops generated after a few cycles of electric field. Also shown are experimental results by Lynch⁹ which were *not* used in the fitting procedure for se-

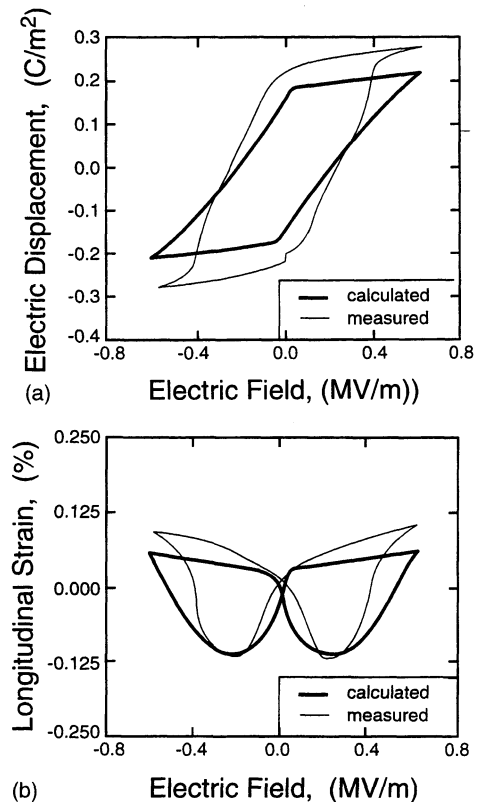


FIG. 5. Simulated and measured 8/65/35 PLZT hysteresis loops produced by applying a cyclic electric field simultaneously with a constant compressive stress of 15 MPa. (a) Electric displacement vs electric field. (b) Longitudinal strain vs electric field.

lecting the values of \bar{E}_0^{90} , \bar{Y} , $\bar{\epsilon}$, and α . Therefore, the calculated curves shown in Figs. 5 and 6 are *predictions* of the experimental loops shown in those plots.

The general features of the hysteresis loop for a constant stress of -15 MPa in Fig. 5(a) are captured quite well in the predicted curves. The process of switching is more gradual than when there is no stress applied. This spreading out of the switching occurs because the applied compression encourages the first of the two consecutive 90° transformations which a crystallite experiences and discourages the second. The remanent polarization is predicted relatively poorly in the calculated curves. This inaccuracy is probably associated with the deficiency of the model in handling stress depolarization, some of which occurs prior to the cycling of the electric field (i.e., the effect of the pre-stress). However, the simulation at a constant stress of -15 MPa underpredicts the remanent polarization magnitude, whereas the stress versus electric displacement simulation curve in Fig. 4 overpredicts the electric displacement magnitude at -15 MPa.

The butterfly loop in Fig. 5(b) at a constant stress of -15 MPa is predicted nicely. The spreading of the switching process by separating the occurrence of the consecutive 90° switches for a given crystallite is indicated clearly by the fatness of the tails of the loop, a feature which is predicted quite well. The remanent strain is reduced considerably compared to the unstressed case because of stress induced depolarization [compare Fig. 5(b) with Fig. 2]. This aspect of the strain behavior is also captured well in the prediction.

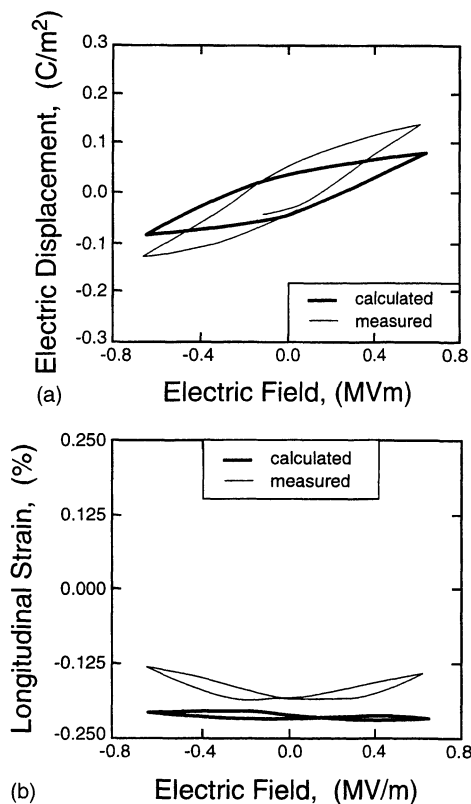


FIG. 6. Simulated and measured 8/65/35 PLZT hysteresis loops produced by applying a cyclic electric field with a constant compressive stress of 60 MPa. (a) Electric displacement vs electric field. (b) Longitudinal strain vs electric field.

The hysteresis loop at a constant stress of -60 MPa as shown in Fig. 6(a) is predicted very well. Both the remanent polarization under compression, much reduced from the unstressed value, and the phenomenon of switching are represented well in the calculated loop. At this stress level, the compression induced depolarization is predicted accurately. The butterfly loop at a stress of -60 MPa shown in Fig. 6(b) indicates that very little 90° switching is going on. The strain loop which occurs is due largely to reversal of the piezoelectric effect which can produce a butterfly loop in the absence of 90° switching.³ Some 90° switching occurs in the loop of Fig. 6(b), and the prediction provides a thinner loop than the experiments.

VII. DISCUSSION

Our model for the behavior of polycrystalline ferroelectric ceramics takes the switching behavior at the crystallite level as the starting point. Crystallites are considered to be entirely polarized in one direction and to switch completely to polarization in another direction when the critical condition for doing so is met. This picture is not entirely satisfactory since it leaves no room for individual domains within the crystallite and glosses over the stage of the process in which domain walls sweep across the crystallite during switching. The accommodation of individual domains in ferroelectrics¹² and other materials²⁹ is important and has been studied. Their presence in ferroelectrics reflects strain and dielectric incompatibilities among neighboring

crystallites¹⁹ and is associated with a significant amount of remanent stored energy. However, from our point of view, the role of domain wall boundary motion is more important. A mean field constraint model for polycrystalline switching, which includes the phenomenon of domain wall motion, could be developed along the lines of that used for plasticity during polycrystalline deformation.^{14,15-18} Such an approach would include the feature that individual grains would have mixtures of domains with different polarizations and would behave as if they were sets of cooperating crystallites as envisioned by Arlt.¹⁹

A fuller treatment of the problem would involve the identification of the relative position in the aggregate of each crystallite and a reasonably accurate calculation of the local electric field, mechanical stress, and average remanent polarization and strain in each crystallite as they progressively switch by domain wall motion. Such a calculation could be carried out by, say, the finite element method. Computations for aggregates containing thousands of crystallites would be very lengthy. Individual constraints on each crystallite would, however, be identified reasonably accurately in such an approach and cooperative switching among neighboring grains would happen naturally. However, until much more thorough treatments of the problem are undertaken, mean field models are of value. The mean field model presented in this article neglects the details of domain wall motion and nearest neighbor interactions among crystallites. Instead, it treats switching in crystallites as an abrupt phenomenon controlled by the applied mechanical and electrical loads constrained by interactions only with the mean field of all other crystallites in the aggregate. However, mean field theories neglect the spatial fluctuations of fields within heterogeneous aggregates and this omission at least affects the details of the results if not the substance.

The model developed in this article has ten disposable parameters. However, three of those are required to match the *linear* response of the experimental material (i.e., Young's modulus, dielectric permittivity, and piezoelectric coefficient) and would be required in any simulation. The other seven parameters are P_0 , e_0 , \bar{E}_0^{90} , \bar{E}_0^{180} , \bar{Y} , $\bar{\epsilon}$, and α , of which P_0 and e_0 are empirical values representing the polarizability and tetragonality of a crystallite. Again, accurate values of these parameters would have to be utilized in any model. Also \bar{E}_0^{180} can be any large value discouraging 180° switches. Therefore, \bar{E}_0^{90} , \bar{Y} , $\bar{\epsilon}$, and α are the only parameters which are used in a phenomenological fashion in the fitting procedure. Notwithstanding this aspect of our approach, we can still assert that \bar{E}_0 (both \bar{E}_0^{90} and \bar{E}_0^{180}), \bar{Y} , and $\bar{\epsilon}$ have a physical meaning. The parameter \bar{E}_0 is an effective value for the coercive field. Indeed, when $\bar{Y}=0$ and $\bar{\epsilon}=\infty$ (as in the simulation carried out by Hwang *et al.*³) the value used for \bar{E}_0 was the experimentally measured level of 0.36 MV/m. In the current approach, with the constraint terms included, \bar{E}_0^{90} is now much less than the empirical coercive field level from the experimental loops. The value used for \bar{E}_0^{90} of 0.13 MV/m is approximately 1/3 of the empirical coercive field value. Our interpretation of this is that switching in an unpoled polycrystal can initiate very easily at

low electric field (i.e., at ~ 0.2 MV/m). However, after significant polarization has developed in the polycrystal, matrix constraint is a significant barrier to switching when the electric field is reversed: the critical field for the second cycle of the electric field is increased from ~ 0.2 to ~ 0.3 MV/m, as in Fig. 1.

The physical interpretations of \bar{Y} and $\bar{\epsilon}$ are as the effective modulus and permittivity of the aggregate associated with the constraint. However, $\bar{Y}=7.5$ GPa is much lower than the crystallite elastic constant of 34 GPa. One interpretation of this aspect of the model (as discussed in Sec. I) is that during switching many crystallites are in the process of transforming, leading to a lowering of the tangent modulus for the polycrystalline aggregate. Similarly, the process in which many crystallites switch simultaneously increases the tangent dielectric permittivity of the polycrystalline aggregate, leading to a high value of $\bar{\epsilon}$ at $0.80 \mu\text{F/m}$ compared to the measured value for the dielectric permittivity of $0.05625 \mu\text{F/m}$. A counterargument to this rationalization is that our model proposes that only one crystallite switches at a time and therefore the full level of linear constraint should be retained by the remaining aggregate. Only if 80% of the crystallites were to switch simultaneously would the constraint be reduced to the level used in the calculations for our model. Another point of view is that the low level of constraint reflects the fact that switching in a heterogeneous aggregate commences near free surfaces, at electrodes, and adjacent to cracks and cavities. These features would reduce the effective level of constraint on crystallites during initial switching. The steepness of experimental hysteresis loops after switching has commenced suggests that our model may be deficient in assuming that only one crystallite switches at a time and that after switching has initiated, low constraint is continued by the simultaneous transformation of many grains.

We offer no physical argument as for why α should be greater than 1 in our simulations. We can only suggest that the value of 1.4 is a consequence of other approximations and assumptions in the model. It is notable that whereas the constraint modulus at 7.5 GPa is about 20% of the true elastic modulus of 34 GPa, the true dielectric permittivity is only about 7% of the constraint permittivity which equals $0.8 \mu\text{F/m}$. This indicates that there is an asymmetry in the adjustments in the model and the enhanced weighting of the potential energy change due to the transformation strain, and can be thought of as a consequence of such asymmetric adjustments and approximations. The omission of piezoelectric terms in the Eshelby calculation of constraint energy for an inclusion probably contributes to this feature as well.

A significant concern is that 8/65/35 PLZT at room temperature is composed mostly of rhombohedral crystallites. (This point came to our attention after the model had been developed and the experiments were complete.) Our model, implemented for tetragonal crystallites, is approximate when applied to rhombohedral materials. (The model can be implemented for rhombohedral crystallites, as it can be for any ferroelectric crystallography. Such a development should be undertaken in the future.) However, the difference between tetragonal symmetry and rhombohedral crystallography is

not great in terms of available switches, spontaneous polarizations, and strains. There is still one 180° switch, but the four 90° switches are replaced by three $\sim 70^\circ$ plus three $\sim 110^\circ$ transformations. Averaged over 5000 crystallites, the four 90° switches per crystallite in the tetragonal implementation of the model are probably quite effective at representing the 70° and 110° switches in the rhombohedral crystallite. A rationalization of our results can be based upon an idea suggested by Arlt.¹⁹ This is that inclusions represent collections of crystallites and therefore can have symmetries other than that of the lattice forming the material.

The accuracy of our results simulating hysteresis, butterfly, and stress-strain loops is reasonable even though the results are not precise. The lack of precision is an indication of the deficiencies in the approach. On the other hand, the relative closeness of the results to the experiments shows the effectiveness of a mean field theory involving complete switching of crystallites and having only ten disposable parameters. Certainly, the introduction of additional disposable parameters or more sweeping *ad hoc* adjustments to the equations would improve the accuracy of the results. For example, Arlt¹⁹ has achieved a very accurate simulation of the charge versus potential hysteresis loops of BaTiO₃ and PLZT using a mean field theory similar to ours. However, he makes an *ad hoc* adjustment to the *form* of the functional expression for the depolarization field in the crystallite to achieve this success. He does not model the strain versus electrical potential butterfly loops, although this could be done readily for BaTiO₃ since there is no remanent strain change in the crystallites in that material. It is notable that Arlt¹⁹ omits the piezoelectric effect on the depolarization field, just as we do.

Rather than change the functional form of terms entering our mean field theory, we prefer to adjust only material constants and then explore the effectiveness of our model, including the prediction of curves not used to choose values for the adjusted parameters. An advantage of our approach is that we are able to provide a prescription for the response of the polycrystal to electrical and mechanical applied fields which are rather different from the simple uniaxial field and stress loadings which are applied to produce hysteresis, butterfly, and stress-strain curves. For example, an electric field could be applied to a previously polarized polycrystal in a direction different from that of the original poling. Whereas, our methodology and material parameters can be used in such a case, we would not know how to extend the model of Arlt to such loadings, nor does he suggest an approach.

Our model is useful for the insight it provides into the constitutive behavior of ferroelectric ceramics and the ability to explore stress and electric field states which are difficult to achieve in the laboratory. While the model could be used as a switching constitutive law for ferroelectric ceramics to carry out stress and electric field analysis of devices and defects, the computational burden of the method is probably too great for such an approach to be effective. Instead, the simulations can be used to guide the development of phenomenological constitutive laws for switching which can be then used more efficiently in device calculations.

ACKNOWLEDGMENTS

This work was supported by ONR through Contract No. N00014-93-1-0200. J.E.H. is grateful for financial support from the EPSRC of the UK and DRA Farnborough. The assistance of Stephen S. Chang in carrying out some modifications to the computer code is acknowledged.

- ¹B. Jaffe, W. R. Cook, and H. Jaffe, *Piezoelectric Ceramics* (Academic, London, 1971).
- ²W. G. Cady, *Piezoelectricity*, (Dover, New York, 1964), Vols. 1 & 2.
- ³S. C. Hwang, C. S. Lynch, and R. M. McMeeking, *Acta Metall. Mater.* **43**, 2073 (1995).
- ⁴K. H. Chan and N. W. Hagood, "Modeling of nonlinear piezoceramics for structural actuation," *Proceedings of SPIE, Smart Structural Materials*, edited by N. W. Hagood (Proc. SPIE 1994), Vol. 2190, p. 194.
- ⁵D. Berlincourt and H. H. A. Krueger, *J. Appl. Phys.* **30**, 1804 (1959).
- ⁶H. H. A. Krueger, *J. Acoust. Soc. Am.* **42**, 636 (1967).
- ⁷H. H. A. Krueger, *J. Acoust. Soc. Am.* **43**, 583 (1968).
- ⁸H. Cao and A. G. Evans, *J. Am. Ceram. Soc.* **76**, 890 (1993).
- ⁹C. S. Lynch, *Acta Mater.* **44**, 4137 (1996).
- ¹⁰E. Fatuzzo and W. J. Merz, *Ferroelectricity* (North-Holland, Amsterdam, 1967).
- ¹¹M. E. Lines and A. M. Glass, *Principles and Applications of Ferroelectrics and Related Materials* (Clarendon, Oxford, 1977).
- ¹²G. Arlt, *Ferroelectrics* **189**, 91 (1996).
- ¹³E. Kroener, *Z. Phys.* **151**, 504 (1958).
- ¹⁴B. Budiansky and T. T. Wu, *Proceedings of the 4th Congress of Applied Mechanics*, 1962, p. 1175.
- ¹⁵R. Hill, *J. Mech. Phys. Solids* **13**, 89 (1965).
- ¹⁶R. Hill, *J. Mech. Phys. Solids* **13**, 213 (1965).
- ¹⁷B. Budiansky, *J. Mech. Phys. Solids* **13**, 223 (1965).
- ¹⁸J. W. Hutchinson, *Proc. R. Soc. London, Ser. A* **319**, 247 (1970).
- ¹⁹G. Arlt, *Ferroelectrics* **189**, 103 (1996).
- ²⁰J. A. Stratton, *Electromagnetic Theory* (McGraw-Hill, New York, 1941).
- ²¹J. D. Eshelby, *Proc. R. Soc. London, Ser. A* **241**, 376 (1957).
- ²²R. M. McMeeking, *Z. Angew. Math. Phys.* **40**, 615 (1989).
- ²³J. D. Eshelby, "Elastic inclusions and inhomogeneities," in *Progress in Solid Mechanics*, edited by I. N. Sneddon and R. Hill (North-Holland Amsterdam, 1961), Vol. II, p. 89.
- ²⁴W. F. Deeg, Ph.D. dissertation, Stanford University, 1980.
- ²⁵Y. Benveniste, *J. Appl. Phys.* **72**, 1086 (1992).
- ²⁶B. Wang, *Int. J. Solids Struct.* **29**, 293 (1992).
- ²⁷M. L. Dunn and M. Taya, *Proc. R. Soc. London, Ser. A* **443**, 265 (1993).
- ²⁸R. M. McMeeking and S. C. Hwang, *Ferroelectrics* **200**, 151 (1997).
- ²⁹J. M. Ball and R. D. James, *Arch. Ration. Mech. Anal.* **100**, 13 (1987).